ACTA IMEKO
ISSN: 2221-870X
June 2018, Volume 7, Number 2, 3-9

High Accuracy Attitude and Navigation System for an Autonomous Underwater Vehicle (AUV)

Enrico Petritoli, Fabio Leccese

Science Department Università degli Studi "Roma Tre" Via Della Vasca Navale n°84, 00146, Rome, Italy

ABSTRACT
This paper examines the development of an attitude and control system for a tailless Autonomous Underwater Vehicle (AUV) without movable control surfaces. As the AUV does not have movable surfaces, the buoyancy system and the center of gravity displacement manage the entire maneuvering system.

Section: RESEARCH PAPER

Keywords: accuracy; attitude; navigation; autonomous; underwater; vehicle; glider; AUV

Citation: Enrico Petritoli, Fabio Leccese, High Accuracy Attitude and Navigation System for an Autonomous Underwater Vehicle (AUV), Acta IMEKO, vol. 7, no. 2, article 2, June 2018, identifier: IMEKO-ACTA-07 (2018)-02-02

Editor: Dušan Agrež, University of Ljubljana, Slovenia

Received January 12, 2018; **In final form** March 21, 2018; **Published** June 2018

Funding: This work was supported by the Science Department of the Università degli Studi Roma Tre, Rome, Italy

Corresponding author: Fabio Leccese, e-mail: fabio.leccese@uniroma3.it

1. INTRODUCTION

The exploration of the sea and the discovery of the sea floor requires a great deal of data and the carrying out of very long research campaigns that can go from a few weeks to several months. For this reason, self-propelled Autonomous Underwater Vehicles (AUVs) are unsuitable because of their too short endurance; the ROVs (Remotely Operated Underwater Vehicle) do not allow a high operative range and therefore require the constant presence of a supporting ship [1].

ALACE was one of the first solutions adopted to solve these problems: a drifting buoy that could suitably regulate its operational depth; once it reached the surface, it transmitted the data collected to the Argos satellite communication system [2].

The need to be free of the randomness of the currents, and the increase of the miniaturization of electronic components, have led to the natural development: the underwater gliders [3].

An underwater glider is an AUV that, by changing its buoyancy, moves up and down in the ocean like a float. Unlike a float, an underwater glider uses hydrodynamic wings to convert the vertical motion to horizontal, moving forward with very low power consumption. Figure 1 shows the example of our AUV called SQUID [4].

2. THE SUB GLIDER

While not so fast as conventional AUVs, sub gliders using buoyancy-based propulsion have a high range and endurance compared to motor-driven vehicles, and may extend the mission to months, and to several thousands of kilometres of

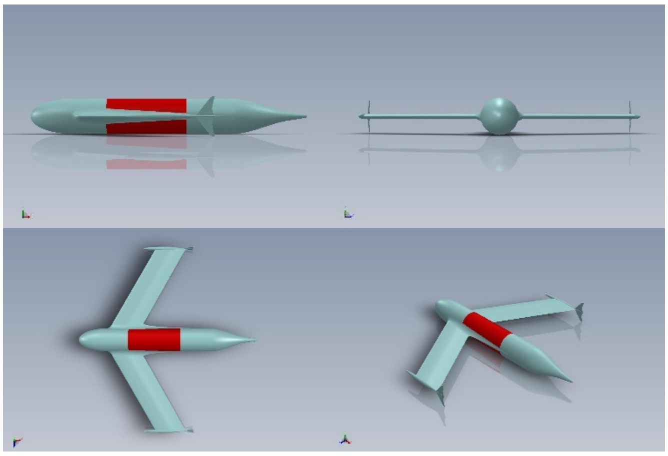

Figure 1. SQUID TUG (Tailless Underwater Glider) view.

range [5].

The SQUID is a tailless sub vehicle: the cylindrical hull has a constant external diameter of 220 mm (approx.), with a radome on the nose and a shaped hydrodynamic fairing in the tail [6].

The hull (fuselage) is made of Aluminium 6061-T6: it has excellent joining characteristics, good acceptance of applied coatings and combines relatively high strength, good workability and high resistance to corrosion [7].

The wings are in Ultem 1000 (Polyetherimide high-density polymer): it has a good dielectric strength, high inherent flame resistance and extremely low smoke generation; furthermore, it has high mechanical properties and performs in continuous use to 170 °C [8].

The vehicle has no movable control surfaces [9].

2.1. Fuselage

The fuselage is composed by five coaxial cylindrical compartments (or bays):

- **Payload Bay**: The nose cone has a prolate hemispheroid shape and contains the (customizable) payload and the ancillary systems, based on the new Raspberry system [10] - [14]. The section up to the first bulkhead is an available space that can be filled with all the needed instrumentation up to a diameter of 200 mm. If an active sonar is required, an alternate version of the radome is available [15]. The second part of the bay accommodates all the ancillary services such as payload power packs, thermal control, and other instrumentation recording and storage devices.
- **Navigation and communications bay**: it contains the Glider Integrated Control System (GICS), the INS (Inertial Navigation System) platform and the radio communication systems (Global Positioning System-GPS, Iridium RTx and HF emergency beacon) [16]. The GICS oversees all the functions of navigation, guidance and vehicle control.
- **Battery bay**: it contains the battery pack and the servomotors to trim and regulate pitch and heading (yaw) of the AUV. The batteries are mounted on a special support (cradle) and actuated by servomotors (controlled by the OBC – On Board Computer) that allow the forward/backward scrolling (for pitch control) but also the right/left tilt for intrinsic direction control (Figure 2).
- **Buoyancy Control Bay:** it contains the buoyancy motor and the oil tank. It balances the system longitudinally by adjusting the level in the reservoir. The bay also supports bulkhead load. The buoyancy motor has the task of pumping oil into the bladder and, in the event of a serious emergency, if ordered by the OBC, it can swell the bladder to the maximum in order to reach rapidly the surface.
- **Hydrodynamic fairing:** it contains the oil bladder, is open to the water and provides a slender shape to the AUV. The fairing has the task of not disturbing the hydrodynamic flow of the fuselage and closing the fuselage in closure. In any case, it must withstand considerable loads: for this reason, there are several reinforcements. It also protects the bladder from the flow and its dynamic loads, which could deform it.

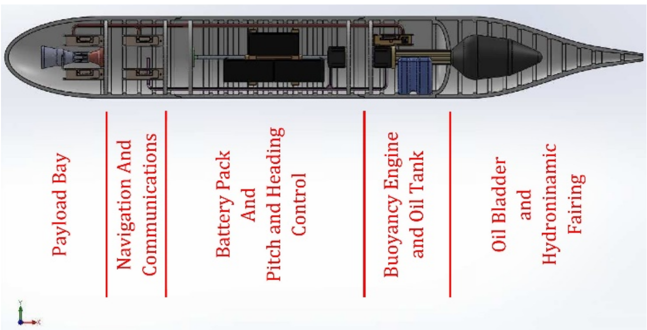

Figure 2. Fuselage profile view (cutaway).

2.2. Wings

The wing has a high aspect ratio with no dihedral and a swept of *Λ* = *30°*: the thickness is constant [17].

The wing profile is symmetric, type *Eppler E838 Hydrofoil* (see Figure 3): it was intended for use at high Reynolds' numbers; the foil is optimized for use as a hydrofoil wing and at low speeds of the AUV it expresses its best lift/drag rate. The choice of such a thick profile is due to two factors: first, the wing is subjected to considerable loads due to the aspect ratio even though the speed remains modest. The second is that in such a thick section it is possible to accommodate a hollow tubular aluminium spar, which increases flexural rigidity.

Each wing tip is provided with a *Küchemann carrot* and a symmetric winglet in order to increase lateral stability and to reduce drag by partial recovery of the tip vortex energy. A *Karman* aerodynamic fitting connects the wing to the fuselage.

3. BUOYANCY SYSTEM

The drone control system is essential: to vary the buoyancy of the vehicle, it is sufficient that the buoyancy motor modifies the quantity (volume) of oil in the bladder: (e.g.) if the overall volume increases, the drone begins to float.

In order to reduce the force required to actuate the oil piston, which pushes the oil in the bladder at high depth, is necessary to reduce the piston surface (diameter) and increase the stroke. So, the buoyancy engine resembles to a "shotgun" [18].

The evaluation of the buoyancy *B* of the drone is made considering the buoyancy of the naked glider (as a rigid body) and the variable component due to the bladder and the buoyancy motor. Therefore, the vertical balance of total forces on the glider is:

$$W_{TOT} = W_{DW} - B_{GB} - B_{BB} \tag{1}$$

where:

W_{TOT} = Net total "weight" in the water.
W_{DW} = *Dry* Weight of the glider.
B_{BB} = Buoyancy of the oil bladder.
B_{GB} = Buoyancy of the naked glider.

4. PITCH CONTROL SYSTEM

For the pitch setting, is necessary to move the battery pack (and therefore the centre of gravity C_G) forward or backward. However, in order to control the heading, it is necessary to tilt

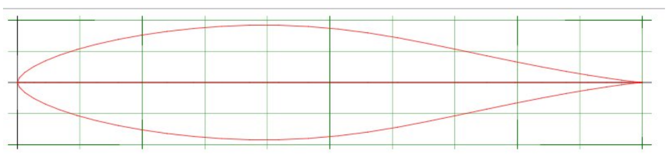

Figure 3. The *Eppler E838 Hydrofoil* profile.

the pack at a certain angle [19].

We have to consider the attitude of the drone with a pitch angle ϑ (see section). For the balance of the forces on the Z-axis, we have (Figure 4):

$$\sum F_z = W_{BA} + W_{OT} + W_{GB} + B_{GB} + B_{BB} = 0 \qquad (2)$$

Where:

W_{BA}= Weight of the battery pack.

W_{OT} = Weight of the oil tank.

W_{GB} = Weight of the naked glider (without oil tank and batteries).

At the equilibrium, we have:

$$\sum M_Y = (l_{BA} + z_{BA}\tan\theta)W_{BA} + l_{OT}W_{OT} + l_{GB}W_{GB} - l_{GB}B_{GB} - l_{BB}B_{BB} = 0 \qquad (3)$$

For the position of the Centre of Buoyancy C^B and the Centre of Gravity C^G we have:

The Centre of Gravity on the X-axis is defined as:

$$C_X^G = \frac{l_{BA}W_{BA}+l_{OT}W_{OT}+l_{GB}W_{GB}}{W_{BA}+W_{OT}+W_{GB}} \qquad (4)$$

The Centre of Gravity on the Z-axis is defined as:

$$C_Z^G = \frac{z_{BA}W_{BA}}{W_{BA}+W_{OT}+W_{GB}} \qquad (5)$$

The Centre of Buoyancy on the X-axis is defined as:

$$C_X^B = \frac{l_{GB}B_{GB}+l_{BB}B_{BB}}{B_{GB}+B_{BB}} \qquad (6)$$

the Centre of Buoyancy on the Z-axis, (by definition):

$$C_Z^B = 0 \qquad (7)$$

5. HEADING CONTROL SYSTEM

To obtain a variation of the heading of the vehicle, due to the absence of the tail, rudder or ailerons, is necessary to move the centre of gravity around of the X-axis [20].

At the equilibrium, for the roll φ angle we have for the roll forces balance (Figure 5):

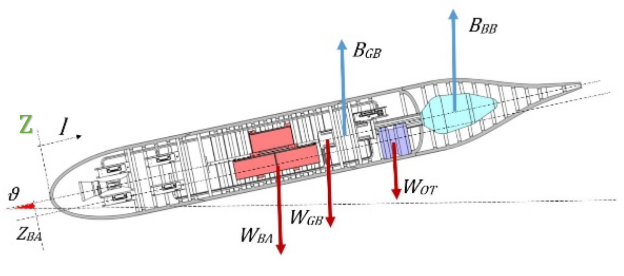

Figure 4. Pitch balance diagram.

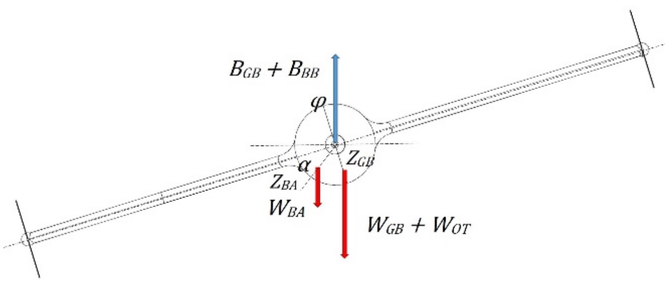

Figure 5. Roll forces balance.

$$\varphi = \frac{z_{BA}\cos\alpha\ W_{BA}}{z_{GB}(W_{GB}+W_{OT})+z_{BA}W_{BA}} \qquad (8)$$

In almost-static conditions, if we move the W_{BA} slowly (or not fast), the only effect is simply the increase of the attitude φ angle. When the AUV is “gliding” (i.e.: diving at constant speed), the effect is completely different. In fact, when the attitude φ angle increases, the up-going wing increases the local angle of attack α_{ATT} so that the lift and the drag increase while the down-going wing reduces the angle of attack, the lift and the drag, producing a rolling (also called 'banking') moment about the aircraft longitudinal axis [20].

In our case, the nose of the drone rotates towards the up-going wing. In particular, the roll motion is characterized by an absence of natural stability; in fact, there are no stability derivatives that generate moments in response to the inertial roll angle (Figure 6).

A roll disturbance induces a roll rate and water viscosity cancels it: this takes place with insignificant changes in some sideslip and a yaw rate.

6. DYNAMIC VERTICAL FORCES BALANCE

Here, we consider the drone diving (or emerging) at constant speed (Figure 7) [21].

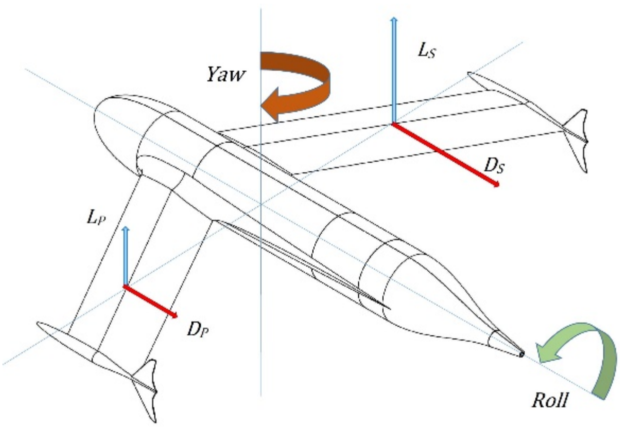

Figure 6. Banking effect scheme.

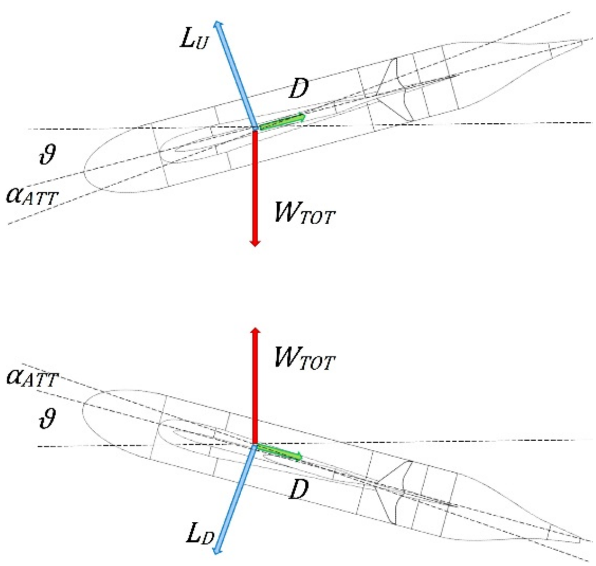

Figure 7. Dynamic vertical forces balance (immersion (top) and emersion (bottom) phases).

At the equilibrium, the dynamics on the vertical plane is, at constant speed:

$$\overrightarrow{W_{TOT}} + \vec{L} + \vec{D} = 0 \tag{9}$$

The expression for the Lift is:

$$L = \frac{1}{2}\rho v^2 S C_L \tag{10}$$

According to the E838 characteristic "*Cl vs. Alpha*" (Figure 8) when the angle of attack $\alpha_{ATT} = 0°$ (is null) the CL is zero so that the lift force L is null.

This shows that the drone cannot progress horizontally at constant speed (straight and level): the only mission profile allowed is a sawtooth curve.

6.1. Glider typical trajectory

Because its motion is due to the difference between the forces of weight and buoyancy, the glider is unable to proceed straight and level, thus being forced to follow a dive/climb trajectory made smooth by the wings [45].

Moreover, unlike gliders in air, AUVs can have ascending glide slopes if the net buoyancy is positive, producing a negative sink rate.

The *buoyancy engine* of the glider allows changing its net buoyancy into alternating positive and negative states, thereby imparting it with the ability to string together a succession of descending and ascending glide slopes referred to as a *sawtooth glide path* (Figure 9).

7. AUV FUNCTIONAL MODES

The particular mission of the AUV allows us to consider it as a simple "Finite-state machine" (FSM). The fundamental normal states of the machine (Figure 10) are essentially two: the

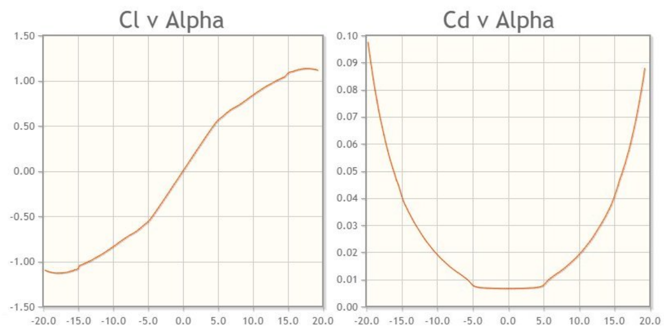

Figure 8. *Eppler E838 Hydrofoil* characteristics (Re = 10^6).

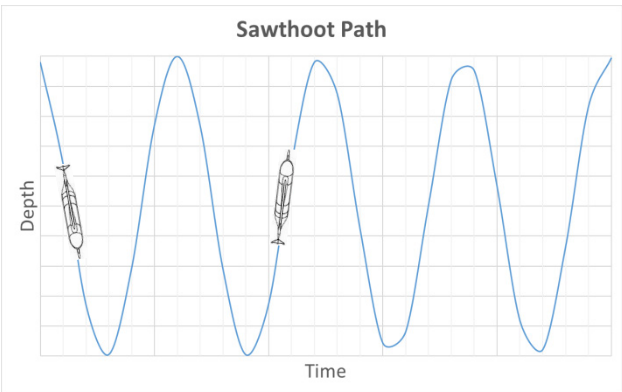

Figure 9. Sawtooth typical glide path (qualitative).

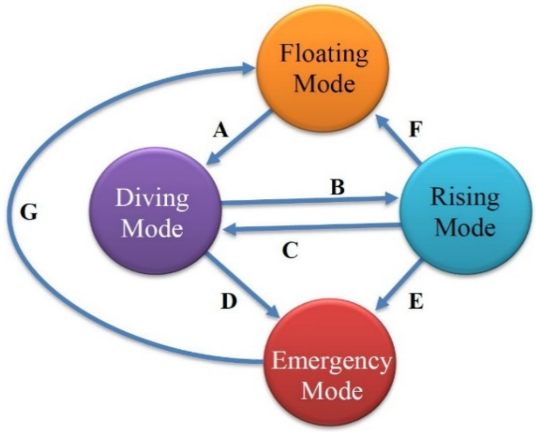

Figure 10. Functional Modes scheme.

"diving mode" and the "rising mode". During these functional modes, the glider describes the sawtooth glide path [23].

The "floating mode" is used only to connect the glider with the support ship and/or used to download payload data through the Satellite communications system. The "emergency mode" manages all possible problems that here we could reassume in dynamic instability, catastrophic failure, loss of batteries, loss of the payload, etc. In this case, the only contemplated action is to bring up the glider for preparing it to be rescued by a support boat [24].

A. Floating Mode

The drone is afloat: at the beginning, from the GPS system, it acquires position coordinates. Then it sends them through another Satellite communication system (e.g. Iridium). Secondly, it waits for a support boat and turn on Wi-Fi for any download of new commands or software update.

B. Diving Mode

The drone is diving: the programmed maximum depth is reached by running the drone at constant speed.

C. Rising Mode

The drone is rising: it proceeds at constant speed until it reaches the programmed minimum depth.

D. Emergency Mode

This is an emergency mode: if an unrecoverable attitude is detected, the system automatically goes to this emergency mode setting the buoyancy to the maximum and placing the trim in the maximum lift. This allows reaching the surface as soon as possible.

E. Transition Conditions

A - The drone receives the command to submerge and to reach the programmed maximum depth.

B - The drone has reached the programmed maximum depth.

C - The drone has reached the programmed minimum depth.

D - An unrecoverable attitude is detected by Attitude System Control.

E - An unrecoverable attitude is detected by Attitude System Control.

F - The drone has ended the mission and receives the command to emerge to wait for new communications.

G - The attitude is trimmed on the maximum ascend ratio and the buoyancy is set to the maximum.

The Glider Integrated Control System (GICS) manages the functional modes status and the transition modes [25].

8. GLIDER INTEGRATED CONTROL SYSTEM (GICS)

The aim of The Glider Integrated Control System is to perform the Attitude and Navigation Control and to manage the Data Handling & Control, including Payload and Communications management functions [26].

The architecture of the GICS is shown in Figure 11. It is built around the Glider Central Unit (GCU), which is a central processing unit and includes several remote terminal units that interface the payload and Glider equipment [27]. The functions performed are:

- Attitude determination and control.
- Buoyancy and other propulsion components control.
- Telemetry data acquisition, formatting and encoding.
- Command detection, decoding, distribution and actuation.
- Battery management.
- Payload Management.

Except for the communications, all other functions are performed when the drone is in autonomous operation [28].

9. NAVIGATION SYSTEM

The navigation system is composed by a Strapdown INS (Inertial Navigation System) system corrected by the GNSS (Global Navigation Satellite System receiver using the GPS, GLONASS, Galileo or BeiDou systems) data every time the vehicle enters in the "floating mode" [29].

All inertial navigation systems suffer from integration drift: small errors in the measurement of acceleration and angular velocity are integrated into progressively larger errors in velocity, which are compounded into still greater errors in position [30].

Since the new position is calculated from the previous calculated position and the measured acceleration and angular velocity, these errors accumulate roughly proportionally to the time since the initial position was input. Therefore, the position must be periodically corrected by input from GNSS (GPS and other) satellite navigation systems when the AUV is in the floating mode [31].

Figure 11. GICS general arrangement.

The benefits of this technology are lower cost, reduced size and greater reliability compared with equivalent platform systems. As a result, small, lightweight and accurate inertial navigation systems may now be fitted to small AUV [32].

The general arranging of an INS is quite simple (Figure 12): the output of a 3-axis accelerometer is rotated (axis transform) with the attitude angles supplied by three gyrometers: after a double integration we have the position offset with respect to the initial point [33].

The incurred major penalties are a substantial increase in computing complexity and the need to use high dynamic range sensors capable of measuring much higher rates of turn.

9.1. INS Errors Assessment

The essential General Error Equations block diagram representation of the error model is given in Figure 13: the diagram shows the Schuler's loop and other cross-coupling terms, which give rise to long-term oscillations [34].

An inertial navigation system over long periods has three type of errors, which propagate in time and are characterized by three distinct frequencies:

- Schuler's oscillation

The Schuler's oscillation has a period of:

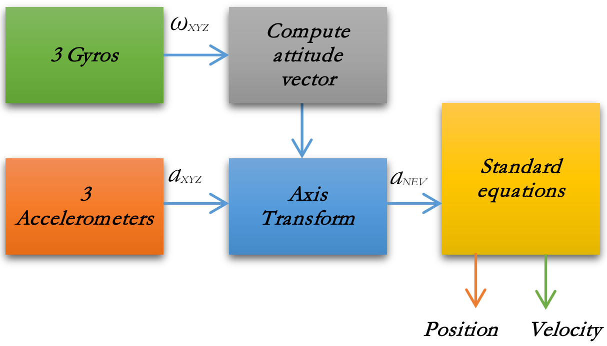

Figure 12. Strapdown INS unit block diagram.

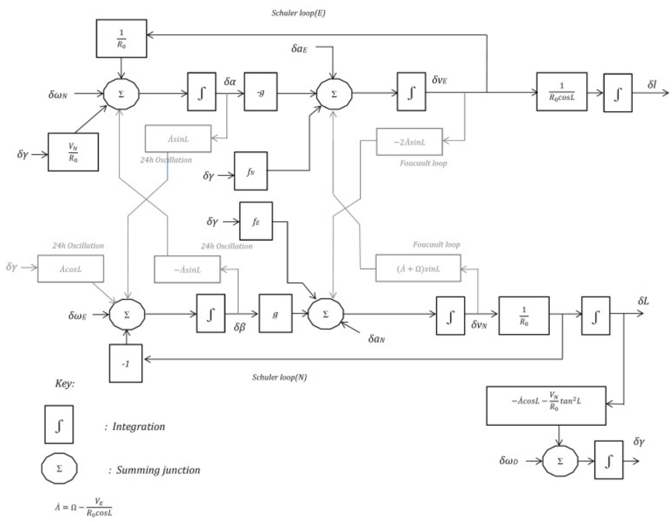

Figure 13. INS long period errors correction block scheme.

$$\omega_s = \sqrt{\frac{g}{R_0}} \qquad T \approx 84.4 \text{ min} \tag{11}$$

and it is present in both horizontal channels.

- Foucault's oscillation

The Foucault's oscillation has a period of:

$$\omega_f = \Omega \sin L \qquad T = \frac{2\pi}{\Omega sinL} \approx 30 \text{ h} \tag{12}$$

and can be considered a modulation of the Schuler's oscillation.

- 24 h Oscillation

The 24 h Oscillation has a period of:

$$\omega_e = 15°/\text{h} \qquad T = 24 \text{ h} \tag{13}$$

and it is obviously equal to the period of rotation of the Earth.

Generally, the full error model in the previous section is required to assess the performance of inertial navigation systems operating for long periods: for our glider applications, flight times are typically of the order of 2-3 days rather than weeks [35].

Unlike an Unmanned Aerial Vehicle (UAV) system, in our case the inertial navigation error terms cannot be neglected: an aerial drone has a rather limited mission time and therefore all long-term oscillation periods can be absolutely deleted in the calculation of the position [36]-[38].

In our case, these errors also have a considerable weight, as they would critically contribute to the *overall* error [39]-[42].

All the following fixes help to minimize the INS platform error: however, at every denomination, the error is cancelled due to the connection to the GNSS system (Figure 14) [43]-[45].

The GNSS measurements are used to update the *Kalman's* filter estimates the INS position, velocity and attitude errors [46]- [47].

These errors are then subtracted from the indicated position, velocity and attitude provided from the INS forming an optimal estimate of the true position [48].

10. CONCLUSIONS

An underwater glider has been presented. For it, we studied both the buoyancy control and the attitude demonstrating that, since the motion equation directly affects the lift force and hence the pitch, it is not possible to separate the buoyancy control system and the attitude control system. In addition, we demonstrated that, during the banking, the speed is directly proportional to the lateral displacement angle of the Centre of Gravity and to the rate of descent.

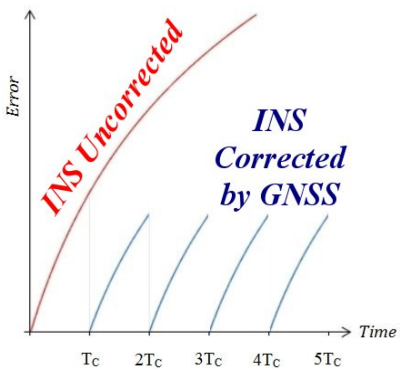

Figure 14. INS Errors Assessment (qualitative).

Given the above, w.r.t. previous similar systems, ours shows the following novelties:

- the presented attitude system control is optimized for a Tailless Underwater Glider with a non-negligible wingspan: in fact, the wide wing surface allows a smooth glide slope and an excellent operational range;
- the AUV has no movable control surfaces in the hydrodynamic flow: therefore, the actuation of the attitude is based only on the variation of buoyancy and on the displacement of the centre of gravity.

Furthermore, a centralized control system called "Glider Integrated Control System (GICS)" was developed for the glider management. The GICS monitors the buoyancy and attitude control (subject of another paper), handles the payload by taking care of the entire data package that it provides and of all communications with the "outside world".

REFERENCES

[1] R.E. Davis, D.C. Webb, L.A. Regier, J. Dufour, "The Autonomous Lagrangian Circulation Explorer (ALACE)", J. Atmos. Oceanic Technol. 9 (1992), pp. 264-285.

[2] S. Wood "Autonomous underwater gliders", in: Underwater Vehicles, Chapter 26, edited by A. V. Inzartsev, 499-524, In-Tech, 2009 Vienna, Austria.

[3] R.W. Beard, T.W. McLain, "Small Unmanned Aircraft - Theory and Practice", Princeton University Press, 2012.

[4] J.S. Wilcox, J.G. Bellingham, Y. Zhang, A.B. Baggeroer, "Performance metrics for oceanographic surveys with autonomous underwater vehicles," IEEE J. Oceanic Eng. 26 (2001), pp. 711-725.

[5] F. Kayton, "Avionics Navigation Systems". Wiley, (1997).

[6] C.C. Eriksen, T.J. Osse, R.D. Light, T. Wen, T.W. Lehman, P.L. Sabin, J.W. Ballard, A.M. Chiodi, "Seaglider: a long-range autonomous underwater vehicle for oceanographic research" Oceanic Engineering, IEEE Journal of, vol. 26 (2001), pp. 424-436.

[7] J.G. Graver. "Underwater Gliders: Dynamics, Control and Design". PhD: Princeton University, 2005.

[8] D.C. Webb, P.J. Simonetti, C.P. Jones, "SLOCUM: An underwater glider propelled by environmental energy", IEEE J. Oceanic Eng. 26 (2001), pp. 447-452.

[9] E. Petritoli, F. Leccese, L. Ciani, "Reliability assessment of UAV systems", Proc. of 4th IEEE International Workshop on Metrology for AeroSpace, MetroAeroSpace 2017, art. no. 7999577, pp. 266-270. DOI: 10.1109/MetroAeroSpace.2017.7999577.

[10] V. Pasquali, G. D'Alessandro, R. Gualtieri, F. Leccese, "A new data logger based on Raspberry-Pi for Arctic Notostraca locomotion investigations", Measurement: Journal of the International Measurement Confederation, 110 (2017), pp. 249-256. DOI: 10.1016/j.measurement.2017.07.004.

[11] F. Leccese, M. Cagnetti, S. Di Pasquale, S. Giarnetti, M. Caciotta, "A new power quality instrument based on raspberry-pi", Electronics (Switzerland) 5 (4) (2016), art. no. 64. DOI: 10.3390/electronics5040064.

[12] V. Pasquali, R. Gualtieri, G. D'Alessandro, F. Leccese, M. Cagnetti, "Experimental in field reliability test for data logger based on Raspberry-Pi for extreme scenarios: A first step versus aerospace applications", Proc. of 3rd IEEE International Workshop on Metrology for Aerospace, MetroAeroSpace 2016, art. no. 7573242, pp. 365-370. DOI: 10.1109/MetroAeroSpace.2016.7573242.

[13] V. Pasquali, R. Gualtieri, G. D'Alessandro, M. Granberg, D. Hazlerigg, M. Cagnetti, F. Leccese, "Monitoring and analyzing of

circadian and ultradian locomotor activity based on Raspberry-Pi", Electronics (Switzerland) 5 (3) (2016), art. no. 58. DOI: 10.3390/electronics5030058.
[14] F. Leccese, M. Cagnetti, A. Calogero, D. Trinca, S. di Pasquale, S. Giarnetti, L. Cozzella, "A new acquisition and imaging system for environmental measurements: An experience on the Italian cultural heritage", Sensors (Switzerland) 14 (5) (2014), pp. 9290-9312. DOI: 10.3390/s140509290.
[15] J. G. Graver, J. Liu, C. Woolsey et al., "Design and Analysis of an Underwater Vehicle for Controlled Gliding," in Conference on Information Sciences and Systems (CISS), Princeton, 1998.
[16] H. Stommel "The Slocum Mission" Oceanography, pp. 22 - 25, April 1989.
[17] J.G. Graver, "Underwater Gliders: Dynamics, Control and Design", PhD thesis, Princeton University, 2005.
[18] J. Sherman, R.E. Davis, W.B. Owens, J. Valdes, "The autonomous underwater glider 'Spray'", IEEE J. Oceanic Eng. 26 (2001), pp. 437-446.
[19] D.L. Rudnick, R.E. Davis, C.C. Eriksen et al., "Underwater Gliders for Ocean Research", Marine Technology Society Journal 38 no. 1. (Spring 2004), pp. 73-84.
[20] D. Titterton, J. Weston "Strapdown Inertial Navigation Technology", 2nd Edition – The Institution of Electrical Engineers and The American Institute of Aeronautics and Astronautics (2005)
[21] A. Pereira, H. Heidarsson, D.A. Caron, B.H. Jones, G.S. Sukhatme, "An implementation of a communication framework for the cost-effective operation of slocum gliders in coastal regions", in Proc. of 7th International Conference on Field and Service Robotics, Cambridge, MA, July 2009.
[22] P. Daponte, L. De Vito, G. Mazzilli, F. Picariello, S. Rapuano, "Method for compensating the effect of disturbances on magnetometer measurements: experimental results", IEEE International Instrumentation and Measurement Technology Conference (I2MTC), 2017, pp. 1 – 6.
[23] D. Küchemann, "The Aerodynamic Design of Aircraft" Pergamon international library of science, technology, engineering, and social studies (1st ed.) 1978. Oxford: Pergamon Press. ISBN 0-08-020515-1.
[24] D. Meyer "Glider Technology for Ocean Observations: A Review", Ocean Sci. Discuss. 2016, doi:10.5194/os-2016-40.
[25] G.Parthasarathy, Degala Shravya Sree, B.Lakshmi Manasa, "Design Mathematical Modeling and Analysis of Underwater Glider", International Journal of Science and Research (IJSR) ISSN (Online): 2319-7064 [QA: year?]
[26] R.E. Davis, C.C. Eriksen, C.P. Jones, "Autonomous buoyancy-driven underwater gliders", in: Technology and Applications of Autonomous Underwater Vehicles, ed. G. Griffiths, pp. 37-58. Taylor and Francis, 2003.
[27] P. Daponte, L. De Vito, G. Mazzilli, F. Picariello, S. Rapuano, M. Riccio, "Metrology for drone and drone for metrology: Measurement systems on small civilian drones", IEEE Metrology for Aerospace (MetroAeroSpace), 2015, pp. 306-311.
[28] C.C. Eriksen, T.J. Osse, R.D. Light, T. Wen, T.W. Lehman, P.L. Sabin, J.W. Ballard, A.M. Chiodi, "Seaglider: A longrange autonomous underwater vehicle for oceanographic research", IEEE J. Oceanic Eng. 26 (2001), pp. 424-436.
[29] D.L. Rudnick et al., "Underwater Gliders for Ocean Research", Marine Technology Society Journal 38 (Spring 2004), no. 1 pp. 41-48.
[30] C.E. Skibski, "Design of an Autonomous Underwater Glider focusing on External Wing Control Surfaces and Sensor Integration", Bachelor of Science Ocean Engineering Florida Institute of Technology, 2009.
[31] S. Chao, J. Caron, L. Sukhatme, "Trajectory Design for Autonomous Underwater Vehicles based on Ocean Model Predictions for Feature Tracking", Field and Service Robotics Volume 62 of the series Springer Tracts in Advanced Robotics 2009, pp 263-273
[32] D. Fontanelli, D. Macii, T. Rizano, "A Fast And Low-Cost Vision-Based Line Tracking Measurement System For Robotic Vehicles", ACTA IMEKO, Vol 4, No 2 (2015) DOI: http://dx.doi.org/10.21014/acta_imeko.v4i2.245
[33] R.N. Smith, M. Schwager, S.L. Smith, D. Rus, G.S. Sukhatme, "Persistent Ocean Monitoring with Underwater Gliders Towards Accurate Reconstruction of Dynamic Ocean Processes", Robotics and Automation (ICRA), 2011 IEEE International Conference.
[34] Techy Tomokiyo Quenzer Beauchamp Morgansen, "Full Scale Wind Tunnel Study of the Seaglider Underwater Glider", UWAA Technical Report September 2010.
[35] C. Waldmann et al., "MOTH-An underwater glider design study carried out as part of the HGF alliance ROBEX," 2014 IEEE/OES Autonomous Underwater Vehicles (AUV), Oxford, MS, 2014, pp. 1-3.doi: 10.1109/AUV.2014.7054401
[36] S.A. Jenkins et al., "Underwater Glider System Study", Scripps Institution of Oceanography, Technical Report No. 53, May 2003.
[37] E. Kureková, M. Omachelová, M. Halaj, Il. Martišovitš, "Positioning Uncertainty of the Tricept Type Parallel Kinematic Structure", ACTA IMEKO, Vol 4, No 4 (2015) DOI: http://dx.doi.org/10.21014/acta_imeko.v4i4.266.
[38] E. Petritoli, T. Giagnacovo, F. Leccese, "Lightweight GNSS/IRS integrated navigation system for UAV vehicles", Proc. of IEEE International Workshop on Metrology for Aerospace, MetroAeroSpace 2014, art. no. 6865894, pp. 56-61. DOI: 10.1109/MetroAeroSpace.2014.6865894.
[39] E. Petritoli, F. Leccese, "Improvement of altitude precision in indoor and urban canyon navigation for small flying vehicles", Proc. of 2nd IEEE International Workshop on Metrology for Aerospace, MetroAeroSpace 2015, art. no. 7180626, pp. 56-60. DOI: 10.1109/MetroAeroSpace.2015.7180626.
[40] X. Xu, X. Xu, T. Zhang, Y. Li, J. Tong, "A kalman filter for sins self-alignment based on vector observation", Sensors (Switzerland) 17 (2) (2017), art. no. 264, DOI: 10.3390/s17020264.
[41] A. Kopacik, P. Kajanek, I. Liptak, "Systematic error elimination using additive measurements and combination of two low cost IMSs", IEEE Sensors Journal 16 (16) (2016), pp. 6239-6248. DOI: 10.1109/JSEN.2016.2581200.
[42] E.L.V. Hinüber, C. Reimer, T. Schneider, M. Stock, "INS/GNSS integration for aerobatic flight applications and aircraft motion surveying", Sensors (Switzerland) 17 (5) (2017), art. no. 941. DOI: 10.3390/s17050941.
[43] Teledyne Webb Research. 2013, "Slocum electric glider". Available at: http://www.webbresearch.com/
[44] I. Bodini, M. Lancini, S. Pasinetti, D. Vetturi, "Techniques for on-board vibrational passenger comfort monitoring in public transport", ACTA IMEKO, Vol 3, No 4 (2014) pp. 197-210
[45] R. Austin "Unmanned Aircraft Systems", Wiley, 2010.
[46] P. Daponte, L. De Vito, F. Lamonaca, F. Picariello, M. Riccio, S. Rapuano, L. Pompetti, M. Pompetti, "DronesBench: an innovative bench to test drones," IEEE Instrumentation & Measurement Magazine, Vol 20, No 6 (2017), pp. 8-15.
[47] F. Lamonaca, D. Luca Carnì, D. Grimaldi, "Time coordination of standalone measurement instruments by synchronized triggering", ACTA IMEKO, Vol 4, No 3 (2015), pp. 23-29.
[48] S. Wood, "State of Technology in Autonomous Underwater Gliders", Marine Technology Society Journal, Volume 47, Number 5, September/October 2013.